J|A|C|S ARTICLES

Published on Web 07/09/2009

Synthesis of Cu-Doped InP Nanocrystals (d-dots) with ZnSe Diffusion Barrier as Efficient and Color-Tunable NIR Emitters

Renguo Xie* and Xiaogang Peng*

Department of Chemistry and Biochemistry, University of Arkansas, Fayetteville, Arkansas 72701

Received May 1, 2009; E-mail: renguoxie@yahoo.com; xpeng@uark.edu

Abstract: Efficient Cu-doped InP quantum dots (Cu:InP d-dots) emitters were successfully synthesized by epitaxial growth of a ZnSe diffusion barrier for the dopants. The Cu dopant emission of the Cu:InP/ZnSe core/shell d-dots covered the important red and near-infrared (NIR) window for biomedical applicaitons, from 630 to 1100 nm, by varying the size of the InP host nanocrystals. These new d-dots emitters not only compensate for the emission wavelength of the existing noncadmium d-dots emitters, Cu- and Mn-doped ZnSe d-dots (450−610 nm), but also offer a complete series of efficient nanocrystal emitters based on InP nanocrystals. The one-pot synthetic scheme for the formation of Cu:InP/ZnSe core/shell d-dots was successfully established by systematically studying the doping process, the dopant concentration-dependent photophysical properties, and the dopant diffusion during shell epitaxy, etc. Complete elimination of InP bandgap emission and efficient pure dopant emission (with photoluminescence quantum yield as high as between 35−40%) of the core/shell d-dots were achieved by optimizing the final doping level and the diffusion barrier thickness.

Introduction

Synthesis of doped semiconductor nanocrystal quantum dots (d-dots)[1−9] have recently become an active subject in the field of materials chemistry because of their unique optical, electronic, and magnetic properties.[10] For example, for the most pursued function of colloidal semiconductor nanocrystals, namely their size-tunable and efficient emission, d-dots[11,12] cannot only retain nearly all advantages of intrinsic quantum dots but also eliminate their self-quenching due to reabsorption/energy transfer, greatly enhance their thermal stability, and significantly improve their chemical stability, etc. In addition, d-dots might also offer high performance emissive materials without any highly toxic Class A elements (Cd, Hg, and Pb) to replace the current workhorse of intrinsic quantum dot emitters, CdSe-based ones. Along this direction, Cu- and Mn-doped ZnSe (Cu:ZnSe and Mn:ZnSe) d-dots were demonstrated as efficient emitters covering the blue to orange color window, with the wavelength below 610 nm.[8] One main goal of the current report was to demonstrate that Cu-doped InP (Cu:InP) d-dots, a different nanocrystal host but still without Class A elements, can be realized as efficient, stable, and tunable emissive materials in red and near-infrared (NIR) windows, approximately between 630 and1100 nm. At present, high performance deep red and NIR emitters[13−15] are much needed for developing desirable probes for in vivo diagnostics and other medical applications.

Despite the recent advancement on synthetic chemistry of colloidal d-dots, successful doping that yielded highly emissive d-dots has been limited to the systems with II−VI semiconductor nanocrystals as the hosts.[1,4,8,11,12,16−20] However, if excluding Cd and Hg as one of the elements, only zinc chalcogenide nanocrystals (typically ZnSe, ZnS, and ZnO) are the possible choices as II−VI semiconductor nanocrystal hosts, which shall have a very limited absorption and emission wavelength range for developing high performance d-dots emitters because of their relatively wide bandgap. Conversely, III−V semiconductor nanocrystals can offer several narrow bandgap hosts without any Class A elements. It has been well-known that synthetic chemistry of intrinsic III−V semiconductor nanocrystals is substantially different from and more difficult than that for

(1) Bhargava, R. N.; Gallagher, D.; Hong, X.; Nurmikko, A. *Phys. Rev. Lett.* **1994**, *72*, 416.
(2) Shim, M.; Guyot-Sionnest, P. *Nature* **2000**, *407*, 981.
(3) Mikulec, F. V.; Kuno, M.; Bennati, M.; Hall, D. A.; Griffin, R. G.; Bawendi, M. G. *J. Am. Chem. Soc.* **2000**, *122*, 2532.
(4) Norris, D. J.; Yao, N.; Charnock, F. T.; Kennedy, T. A. *Nano Lett.* **2001**, *1*, 3.
(5) Radovanovic, P.; Gamelin, D. R. *J. Am. Chem. Soc.* **2001**, *123*, 12207.
(6) Hanif, K. M.; Meulenberg, R. W.; Strouse, G. F. *J. Am. Chem. Soc.* **2002**, *124*, 11495.
(7) Yang, H.; Holloway, P. H. *Appl. Phys. Lett.* **2003**, *82*, 1965.
(8) Pradhan, N.; Goorskey, D.; Thessing, J.; Peng, X. G. *J. Am. Chem. Soc.* **2005**, *127*, 17586.
(9) Yang, Y.; Chen, O.; Angerhofer, A.; Cao, Y. C. *J. Am. Chem. Soc.* **2006**, *128*, 12428.
(10) Norris, D. J.; Efros, A. L.; Erwin, S. C. *Science* **2008**, *319*, 1776.
(11) Pradhan, N.; Peng, X. G. *J. Am. Chem. Soc.* **2007**, *129*, 3339.
(12) Pradhan, N.; Battaglia, D.; Liu, Y.; Peng, X. G. *Nano Lett.* **2007**, *7*, 312.
(13) Kim, S.; Lim, Y. T.; Soltesz, E. G.; De Grand, A. M.; Lee, J.; Nakayama, A.; Parker, J. A.; Mihaljevic, T.; Laurence, R. G.; Dor, D. M.; Cohn, L. H.; Bawendi, M. G. *Nat. Biotechnol.* **2004**, *22*, 93.
(14) Gao, X. H.; Cui, Y. Y.; Levenson, R. M.; Chung, L. W. K.; Nie, S. M. *Nat. Biotechnol.* **2004**, *22*, 969.
(15) Xie, R. G.; Chen, K.; Chen, X. Y.; Peng, X. *Nano Res.* **2008**, *1*, 457.
(16) Sooklal, K.; Cullum, B. S.; Angel, S. M.; Murphy, C. *J. Phys. Chem.* **1996**, *100*, 4551.
(17) Counio, G.; Esnouf, S.; Gacoin, T.; Boilot, J. P. *J. Phys. Chem.* **1996**, *100*, 20021.
(18) Bol, A. A.; Meijerink, A. *J. Phys. Chem. B* **2001**, *105*, 10203.
(19) Azad Malik, M.; O'Brien, P.; Revaprasadu, N. *J. Mater. Chem.* **2001**, *11*, 2382.
(20) Yang, Y.; Chen, O.; Angerhofer, A.; Cao, Y. C. *J. Am. Chem. Soc.* **2008**, *128*, 12428.

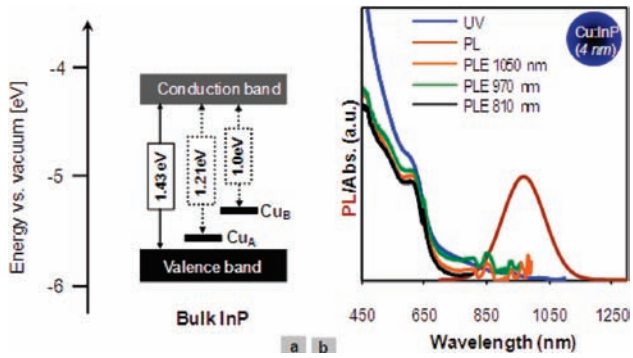

Figure 1. (a) Schematic illustration of the energy diagram of Cu-doped bulk InP crystals. (b) UV−vis, PL, and PLE spectra 4 nm Cu:InP d-dots.

II−VI ones.[21−23] As for III−V d-dots, the knowledge has been quite limited. Several papers reported growth of Mn-doped III−V semiconductor nanocrystals for spintronics purposes, and the resulting d-dots only showed bandgap emission.[24,25] Thus, the second main goal of this work was to explore the unique doping chemistry of III−V semiconductor nanocrystals using Cu:InP d-dots as the model system.

The third main goal of this work was to study synthetic strategy for combating the high mobility of the dopant ions in d-dots at a typical growth temperature. For instance, the critical temperature of diffusion was found at about 230 °C for Cu:ZnSe d-dots,[26] opposite to 580 °C for the corresponding bulk system.[27] When the dopants diffused to the position within the "mean free path of diffusion" from the surface of a nanocrystal, they could be readily ejected from the nanocrystal host through a process called "lattice ejection" occurring at even lower temperatures, below 100 °C for Cu:ZnSe d-dots.[26] Different from the zinc/cadmium (host cations) and copper/manganese (dopant cations) in the previously studied II−VI based d-dots, copper (dopant cations) and indium (host cations) in Cu:InP d-dots would not be isoelectronic. Consequently, diffusion of dopant ions and other related processes in such d-dots systems might be more difficult to control.[24]

Although high performance colloidal Cu-doped III−V d-dots emitters have not been reported yet, Cu-doped III−V semiconductor materials were conducted by a physical method with bulk crystals and solid films, and two dominant Cu-related photoluminescence bands in InP[28,29] were observed at 1.21 eV and 1.01 eV (Figure 1a), respectively. Similar to the Cu-doped ZnSe system,[8] the emission in the Cu:InP system originates from the radiative recombination of electrons from the conduction band of the host and the holes located in the dopant ions, which implies that Cu:InP d-dots have a potential to yield color-tunable emission in a broad optical window. These facts bring a bright perspective for developing Cu:InP d-dots as highly efficient and color-tunable emitters in the red and NIR window.

Results and Discussion

Photoluminescence (PL) related to copper dopants in bulk InP lattice was reported in literature through diffusion of Cu into InP thin films. At about 300 °C, a single PL band at 1.2 eV related to Cu A energy level started to appear and, at about 600 °C, both Cu A (1.2 eV) and Cu B (1.0 eV) PL bands were observed.[28,29] A schematic energy diagram of Cu-doped bulk InP is presented in Figure 1a. These existing knowledge in the bulk system has two interesting implications. First, the emission is a result of the electrons located at the bottom of the conduction band of the host and the hole localized in the dopant centers. Consequently, the emission peak should be tunable by varying the size of the host nanocrystals and, at the same time, it should be possible to capture all advantages of typical dopant emission, such as zero self-quenching, outstanding thermal stability, and improved chemical stability.[11,12] Second, the diffusion temperature of Cu ions in InP bulk lattice[30] seems to have a relatively low temperature in comparison to that in ZnSe bulk lattice.[27,30] Therefore, the critical temperature of lattice diffusion in InP nanocrystals should be lower than that of the Cu:ZnSe d-dots system (230 °C),[26] which should in turn require a relatively low reaction temperature for Cu doping in InP nanocrystals.

Figure 1b presents UV−vis, PL, and PL excitation (PLE) spectra of Cu:InP d-dots (∼4 nm in size). As described in the Experimental Section, the Cu:InP d-dots were obtained by reacting the preformed intrinsic InP dots with the Cu dopant precursor at 180 °C in one pot. As expected, the InP bandgap PL diminished and the PL spectrum was dominated by a band centered at 950 nm. It should be noticed that the bulk bandgap of InP is 1.43 eV (Figure 1a), or 867 nm, which means that the PL peak in Figure 1b could not be the bandgap emission of intrinsic InP nanocrystals. The substantial energy gap between the absorption peak and PL peak in Figure 1b further supports that the PL should be the targeted Cu dopant PL. In practice, this large energy gap is the basis of zero self-quenching of the Cu:InP d-dots because negligible reabsorption can occur for the d-dots.

PLE measurements (Figure 1b) indicate that PL at a different wavelength in the broadband had similar excitation spectra, which means that this broadband was indeed not due to the size distribution of the nanocrystals. This further supports the broadening due to the coexistence of both Cu A and Cu B bands in a PL spectrum of Cu:InP d-dots. Also consistent with this, the full width at half-maximum of the PL spectrum in Figure 1b (0.24 eV) is quite close to the energy difference between Cu A and Cu B energy levels (0.21 eV). It should be pointed out that, because the electrons come from the conduction band of the host (Figure 1a), the size distribution of the host nanocrystals could further broaden the Cu dopant PL spectra. Consequently, the energy difference between Cu A and Cu B bands only offered the low limit of the full width at half-maximum of all PL spectra in Figure 2a. With this evidence, one would conclude that it might be difficult to synthesize Cu:InP d-dots with a PL band as narrow as that of an intrinsic InP quantum dots (q-dots) sample.

With the above results, it is safe to claim that the broad PL band (Figure 1a and Figure 2, top panel) implies that at 180

(21) Micic, O. I.; Sprague, J. R.; Curtis, C. J.; Jones, K. M.; Machol, J. L.; Nozik, A. J.; Giessen, H.; Fluegel, B.; Mohs, G.; Peyghambarian, N. *J. Phys. Chem.* **1995**, *99*, 7754.
(22) Xie, R. G.; Battaglia, D.; Peng, X. G. *J. Am. Chem. Soc.* **2007**, *129*, 15432.
(23) Xie, R. G.; Peng, X. G. *Angew. Chem., Int. Ed.* **2008**, *47*, 7677.
(24) Somaskandan, K.; Tsoi, G. M.; Wenger, L. E.; Brock, S. L. *Chem. Mater.* **2005**, *17*, 1190.
(25) Poddar, P.; Sahoo, Y.; Srikanth, H.; Pradhan, N. *Appl. Phys. Lett.* **2005**, *87*, 3.
(26) Chen, D.; Viswanatha, R.; Ong, G.; Xie, R. G.; Balasubramaninan, M.; Peng, X. G. *J. Am. Chem. Soc.* **2009**, *131*, 9333.
(27) Aven, M.; Halsted, R. E. *Phys. Rev.* **1965**, *137*, 228.
(28) Skolnick, M. S.; Dean, P.; Pitt, A.; Uihlein, C.; Krath, H.; Deveaud, B.; Foulkes, E. J. *J. Phys. C: Solid State Phys.* **1983**, *16*, 1967.
(29) Pal, D.; Bose, D. N. *J. Electron. Mater.* **1996**, *25*, 677.
(30) Kullendorff, N.; Jansson, L.; Ledebo, L. A. *J. Appl. Phys.* **1983**, *54*, 3203.

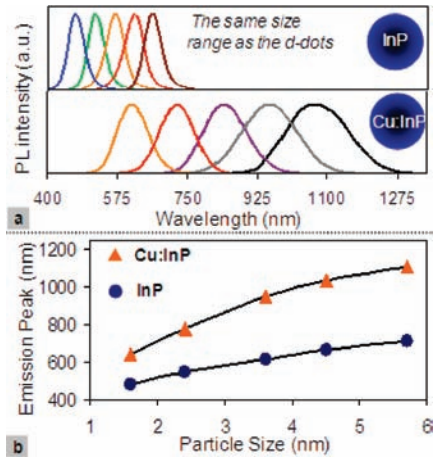

Figure 2. PL spectra (a) and PL peak positions (b) of differently sized InP q-dots and Cu:InP d-dots.

°C, both Cu A and Cu B bands (Figure 1a) were activated for the resulting d-dots. This temperature is substantially lower than 300 °C for observing any Cu dopant PL (only the Cu A band) and 600 °C for obtaining both Cu A and Cu B bands in bulk InP.[28−30]

Color-tunable Cu dopant PL in red and NIR window in Cu:InP d-dots was realized by changing the size of InP host nanocrystals (Figure 2). This optical window, from 630 to 1100 nm, compensates for the missing emission wavelength of the current existing high performance non-cadmium d-dot emitters (Cu:ZnSe and Mn:ZnSe ones), which ended at about 610 nm.[8] Furthermore, the wavelength window of the Cu:InP d-dots also covers the entire NIR window interested for in vivo imaging in various biomedical applications. For such applications, it would be ideal to have a relatively small physical size of the nanocrystals (<10 nm) for a better physical permeability,[15] which should be readily achievable with these relatively small Cu:InP d-dots (Figure 2, bottom).

For comparison, the PL spectra of the intrinsic InP quantum dots (q-dots) in the same size range of the d-dots are also presented in Figure 2a. The two sets of PL spectra in Figure 2a not only illustrate the peak position and width difference between the d-dots and q-dots emitters but also reveal a possibility to cover nearly the entire visible and NIR optical window by InP-based nanocrystals, approximately from about 450 to 1100 nm. Practically, as to be discussed below, the synthetic schemes of the Cu:InP d-dots and the intrinsic InP q-dots were quite similar.[22]

Reaction temperatures were suspected to be a key factor in successful doping of InP nanocrystals. As demonstrated in Cu:ZnSe and Mn:ZnSe d-dots systems,[26] a doping process actually includes multiple elementary (or quasielementary) steps, such as surface adsorption/desorption, lattice incorporation/ejection, and lattice diffusion.

In order to determine an optimal temperature profile for the formation of high quality Cu:InP d-dost system, systematic studies of the doping processes were studied using the established methods,[26] which targeted to identify the optimal choice of the reaction temperatures for different doping stages. The typical results shown in Figure S1 (Supporting Information) indicate that the "surface adsorption" of Cu ions onto the InP host nanocrystals occurred at room temperature in the current system. In the experiment shown in Figure S1 (Supporting Information), "surface adsorption" was completed within 50 min

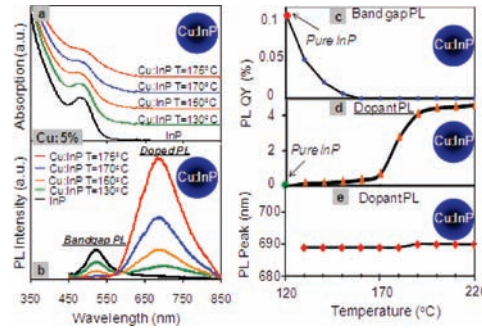

Figure 3. UV−vis (a), PL spectra (b), InP bandgap PL quantum yield (c), Cu dopant PL quantum yield (d), and Cu dopant PL peak position (e) of Cu:InP d-dots at different reaction temperatures. It took 5 min for the reaction to increase the temperature from one point to the next one in c, d, and e.

at 50 °C, indicated by the complete quenching of the InP bandgap PL. However, "lattice incorporation" did not occur until the temperature was higher than about 110 °C (Figure S1), which resulted in the graduate appearance of the Cu dopant PL. In the temperature between 175 and 200 °C, a dramatic increase of the dopant PL intensity was observed, which was found to be even about 1−2 magnitudes higher than that of the original bandgap PL of the corresponding intrinsic InP nanocrystals (see Figure 3c and 3d for quantitative comparison). A plausible explanation of this dramatic increase of dopant PL could be the diffusion of the dopant ions from the surface lattice partially into the interior of the host nanocrystals ("lattice diffusion"), which isolated the emission centers from the surface traps.

On the basis of the above observations, 130 °C was chosen as the temperature for the addition of copper precursor for an efficient but still controlled surface adsorption of the dopant ions. After the formation of intrinsic InP nanocrystals following the published method,[22] the reaction solution was adjusted to 130 °C for the addition of the copper precursors for the surface adsorption. Subsequently, the reaction solution was heated up in a rate of 2 °C/min.

Figure 3a,b illustrates the temporal evolution of UV−vis and PL spectra for a typical reaction with the average size of the intrinsic InP nanocrystals being about 1.8 nm and UV peak position at about 470 nm. As the reaction proceeded, the first excitonic absorption peak of the intrinsic InP nanocrystals became less pronounced gradually although the peak position did not change. Simultaneously, a tail at the long wavelength side of the first excitonic peak appeared. Although the nanocrystals of this specific reaction could not be observed using TEM, the TEM measurements revealed there was no significant size and size distribution variation in such a process using large InP nanocrystals. Furthermore, similar spectroscopic changes were reproducibly detected even at room temperature upon the addition of copper precursors into the InP q-dots solution, again without changing the size distribution of the nanocrystals. We noticed that such spectroscopic changes are consistent with electronically doping semiconductor nanocrystals.[2] Thus, one tentative explanation of such spectroscopic changes could be a result of replacing trivalent indium ions by bivalent copper ions. More systematic studies are needed to definitely explain these interesting spectroscopic changes.

All of the changes in UV−vis absorption mentioned in the above paragraph were accompanied by the decrease of the intensity of the bandgap PL without changing the PL peak position and peak width (Figure 3b). Consistent with the results

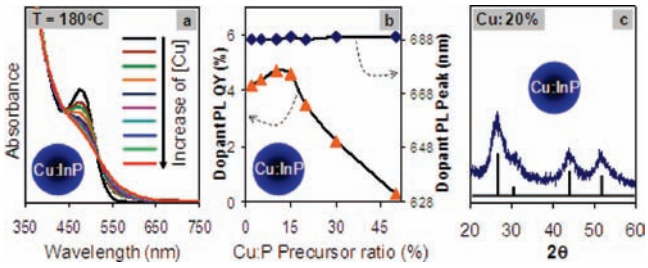

Figure 4. (a) UV−vis absorption spectra of Cu:InP d-dots with different copper concentration (from 0% (top) to 50% (bottom)). (b) The dopant PL QY and peak position of the corresponding samples in part a. (c) XRD pattern of one sample of Cu:InP d-dots with a doping level of 20%.

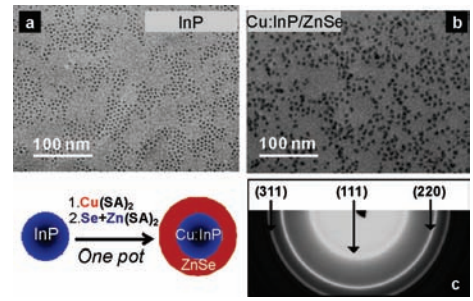

Figure 5. TEM images of InP core (a) and Cu:InP/ZnSe core/shell d-dots (b), electron diffraction pattern of the sample associated with part b.

in Figure S1 (Supporting Information), the broad dopant PL peak started to increase its intensity as diminishing of the bandgap PL decreased, and the dramatic intensity increase of the dopant PL occurred in the expected temperature range (Figure 3d). After the sharp increase in intensity, the dopant PL became stable until the temperature reached about 255 °C. At 255 °C the dopant PL intensity started to decrease, the peak position shifted to red, and the UV−vis absorption spectrum became featureless, which all indicated the occurrence of Ostwald ripening in this high temperature range (Figure S2, Supporting Information).

The results discussed in the above paragraph not only offered a guidelines for growing Cu:InP d-dots with a relatively high PL brightness, about 45 times brighter than that of the bandgap PL of the original InP host nanocrystals (Figure 3c and 3d), but also revealed that the dramatic dopant PL increase between 175 and 200 °C was independent of the heating profile (comparing the results in Figure 3d and Figure S1). This further indicates that this "lattice diffusion" step is an intrinsic step and could be decoupled from the "surface adsorption" and "lattice incorporation" steps. As reported recently,[26] the loosely adsorbed dopant ions on the surface of host nanocrystals through "surface adsorption" quenches the bandgap PL of the host nanocrystals but does not behave as emission centers. "Lattice incorporation" should enable weak dopant PL because the dopant ions were only incorporated into the lattice close to the surface of the host nanocrystals. If this step should be the "lattice diffusion" of the dopant ions, it also means that the critical temperature for lattice diffusion for Cu:InP d-dots system would be about 180−190 °C, which is substantially lower than that for both Cu:ZnSe and Mn:ZnSe d-dots systems, in the range between 220 and 260 °C.[26]

The effects of dopant concentration on the optical properties of d-dots were studied systematically under the same reaction conditions (Figure 4). Figure 4a illustrates the UV−vis spectra of Cu:InP d-dots formed by varying the Cu:P precursor ratio at 180 °C. With increasing the relative concentration of Cu precursor in the solution, the first excitonic absorption peak of the intrinsic InP q-dots (the black line in Figure 5a) became more and more smeared. At the same time, the long tail at the long wavelength side appeared in Figure 3a became more and more pronounced. These trends were noticed to be consistent with the features associated with electronic doping of semiconductor nanocrystals as discussed above (see Figure 3a and the related text).[2]

While the dopant PL peak position and spectral contour were found be independent of the Cu precursor concentration in the solution, the PL QY showed a maximum at about 10% of Cu concentration (relative to the initial concentration of P precursor, the limiting reagent in the system for the formation of InP nanocrystals) as shown in Figure 4b. Energy dispersive spectroscopy (EDS) measurements revealed that the atomic composition of the resulting d-dots had a value similar to that of the ratios of the precursors (see details in the core/shell subsection). The size of the InP dots used in this set of experiments was about 1.8 nm, which has about 55 InP structural units in each nanocrystal. A 10% dopant level means about five to six dopant ions per nanocrystal on average, which approximately matched the optimal value observed for Cu:ZnSe d-dots (six copper atoms per particle).[26]

A high level of dopants was usually hard to reach and might change the lattice structure of the host materials. To confirm that the crystal lattice of the InP host nanocrystals was intact, the XRD pattern of a d-dot sample with a relatively high doping level, 20%, is shown in Figure 4c. For comparison, the diffraction peaks of bulk InP crystals were marked as solid lines in Figure 4c. Evidently, the d-dots diffraction pattern matched well with the expected one, which indicates that a high level doping did not change the lattice structure of the host InP nanocrystals. For different dopant levels, electron diffraction patterns were examined routinely, and the resulting diffraction patterns were found also to be consistent with that of cubic InP crystal lattice.

A one-pot synthesis of Cu:InP/ZnSe core/shell d-dots was developed for improving both the chemical stability and optical performance of the Cu:InP d-dots. As mentioned in the introduction, d-dots are more stable and durable in comparison to their corresponding q-dots. For the current system, Cu:InP d-dots, presumably within their dopant centers located in the interior of the d-dots upon lattice diffusion, were found to possess a much higher PL QY than the intrinsic InP q-dots could possess (see Figure 3c, 3d, and the related text). Furthermore, the bandgap PL of intrinsic InP q-dots was quenched within minutes after they were exposed to air. Conversely, the dopant PL of the Cu:InP d-dots could last for hours in air. However, although improved in comparison with the q-dots, Cu:InP d-dots were neither efficient nor stable in terms of practical applications. Furthermore, growth of pure InP onto the d-dots did not improve their optical properties. In fact, the results indicate that the Cu dopants were readily excluded from the d-dots upon the growth of pure InP. (Figure S3, Supporting Information).

A one-pot approach for the synthesis of Cu:InP/ZnSe core/shell d-dots was developed on the basis of the existing synthetic scheme of the InP nanocrystals[22] (Figure 5) in hope that the ZnSe shell shall not only improve the chemical stability of the d-dots but also provide a diffusion barrier for the dopant ions. ZnSe was chosen as the shell material because we noticed that successful growth of Cu:ZnSe d-dots by overcoating core- and surface-doped ZnSe nanocrystals with ZnSe shell was developed

in the past.[8] We suspected that the ZnSe lattice might be substantially more suited for stabilizing the Cu dopant ions. It should be pointed out that although there is no report on core/shell d-dots based on III−V hosts, results on core/shell d-dots with CdS nanocrystals as the hosts, such as Mn:CdS/ZnS core/shell d-dots,[7,9,20] were investigated by different research groups.

SILAR and thermal cycling techniques[31−33] were employed to grow ZnSe shell onto Cu:InP d-dots (see Experimental Section for details). To do so, a calculated amount of Zn and Se precursors were added into the reaction solution in an alternative fashion at 190 °C, and then the reaction mixture was heated up to about 220 °C needed for the growth of the ZnSe shell. Upon the growth of the core/shell nanocrystals, an apparent increase in size of the nanocrystals was identified using TEM measurements (Figure 5a and 5b), and the resulting core/shell d-dots were found to have a single set of diffraction rings with a zinc blend lattice (Figure 5c), which is consistent with the successful growth of the ZnSe shell onto the existing Cu:InP d-dots. High resolution TEM pictures (Figure S4, Supporting Information) showed the lattice fringes of the resulting nanocrystals across the entire nanocrystal as expected for epitaxial growth. Furthermore, upon the growth of first three monolayers of the ZnSe shell, the UV−vis spectra of the d-dots noticeably shifted red (Figure S5Supporting Information), which also implies the epitaxial growth of the core/shell structures instead of alloy formation.[34]

Although the shape and size distribution of core/shell d-dots still had some room for further improvement, the optical quality of the resulting core/shell d-dots, such as PL QY, photostability, and excitation wavelength, has improved to a level comparable with typical noncadmium NIR emitters of intrinsic core/shell q-dots[35,36] used for in vivo biolabeling.[13−15] The Cu:InP/ZnSe core/shell d-dots showed a 10 times higher dopant PL QY than that of the original Cu:InP d-dots, as high as being close to 40% (Figure 6). The core/shell d-dots were found to be stable when stored under ambient conditions for months.

The optical properties of the Cu:InP/ZnSe core/shell d-dots were found to be strongly dependent on the Cu concentration in the initial Cu:InP core d-dots. For a relatively low Cu:P ratio (Figure 6a), upon the growth of the ZnSe shell, the dopant PL intensity increased initially but started to decrease steadily after the ZnSe shell was more than two monolayers. Simultaneously, the InP bandgap emission started to appear (Figure 6a). It should be pointed out that the appearance of the InP bandgap PL was unlikely in the formation of new q-dots. As shown in Figure S6 (Supporting Information), PLE measurements indicate that both PL peaks in one sample gave almost identical PLE spectra, indicating that both bandgap PL and dopant PL were originated from the same set of InP host nanocrystals. These results suggest that, during the growth of the ZnSe shell, some of the d-dots became q-dots by excluding copper ions from their lattice. This hypothesis was confirmed by examining the final Cu concentration in the resulting core/shell d-dots (Figure 6d and more discussions below).

(31) Li, J. J.; Wang, Y. A.; Guo, W. Z.; Keay, J. C.; Mishima, T. D.; Johnson, M. B.; Peng, X. G. *J. Am. Chem. Soc.* **2003**, *125*, 12567.
(32) Xie, R. G.; Kolb, U.; Li, J.; Basche, T.; Mews, A. *J. Am. Chem. Soc.* **2005**, *127*, 7480.
(33) Blackman, B.; Battaglia, D. M.; Mishima, T. D.; Johnson, M. B.; Peng, X. G. *Chem. Mater.* **2007**, *19*, 3815.
(34) Peng, X. G.; Schlamp, M. C.; Kadavanich, A. V.; Alivisatos, A. P. *J. Am. Chem. Soc.* **1997**, *119*, 7019.
(35) Allen, P. M.; Bawendi, M. G. *J. Am. Chem. Soc.* **2008**, *130*, 9240.
(36) Xie, R. G.; Rutherford, M.; Peng, X. G. *J. Am. Chem. Soc.* **2009**, *131*, 5691.

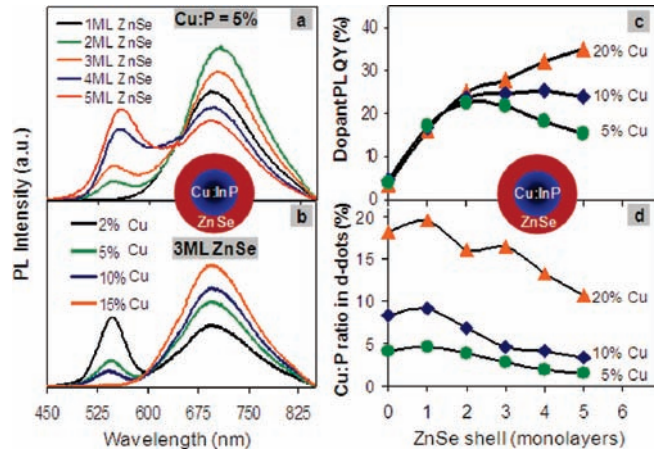

Figure 6. (a) PL spectra of Cu:InP d-dots (formed with 5% of Cu:P precursor ratio) with different thicknesses of ZnSe shells. (b) PL spectra of Cu:InP/ZnSe core/shell d-dots (three monolayers for ZnSe) formed with different Cu:P precursor ratios for the Cu:InP cores. (c) Dopant PL QY of d-dots vs the ZnSe shell thickness with a different initial Cu:P precursor concentration. (d) The Cu concentration in the Cu:InP/ZnSe core/shell d-dots vs the ZnSe shell thickness with a different initial Cu:P precursor concentration.

Fortunately, the problem mentioned in the above paragraph could be solved by introducing more Cu dopant ions into the Cu:InP core d-dots prior to the shell epitaxy. Figure 6b shows that the PL spectra of Cu:InP/ZnSe core/shell d-dots, all after growth of three monolayers of the ZnSe shell under the same reaction conditions, showed systematic reduction of the bandgap contribution upon increasing the Cu concentration in the core d-dots. Significantly, when the Cu concentration increased to 15%, the bandgap PL was eliminated completely.

More systematic and quantitative studies on the PL properties of Cu:InP/ZnSe core/shell d-dots are summarized in Figure 6c and 6d. At a high Cu concentration (20% of the total cations of the core), the dopant PL QY increased steadily upon the ZnSe shell thickness increased, from about 3% to about 35% for this specific reaction. The dopant PL QY of the medium Cu concentration (10% of the total cations of the core) showed a plateau (∼20% PL QY) after two ZnSe monolayers were grown onto the d-dots. As for the reaction with a low Cu concentration (5% of the total cations of the core), the dopant PL QY actually showed a significant trend of drop after the ZnSe shell was thicker than two monolayers. Shown in Figure 6b, two reactions with both medium and low Cu concentrations started to show a significant bandgap PL for the core/shell dots with the growth of three monolayers of ZnSe shell under elevated temperatures.

The results in Figure 6d revealed that, for all three reactions, the Cu concentration found in the resulting d-dots after careful purification from the reaction mixture (see Experimental Section) decreased steadily as the shell thickness increased. This quantitatively confirmed the elimination of Cu dopant ions from the resulting core/shell d-dots (Table S1, Supporting Information). Upon growing five monolayers of ZnSe on average, the Cu concentration dropped about 50%. Interestingly, the final Cu concentration for the core/shell d-dots with the highest dopant PL QY in Figure 6c was about 10% of the total cations in the core nanocrystals, which is consistent with the optimal Cu concentration for achieving maximum dopant PL QY for Cu:InP core d-dots revealed by Figure 4b.

To summarize the results of Figure 6, we concluded that Cu dopant ions were eliminated from the nanocrystal lattice upon the growth of the ZnSe shell. This elimination could not be

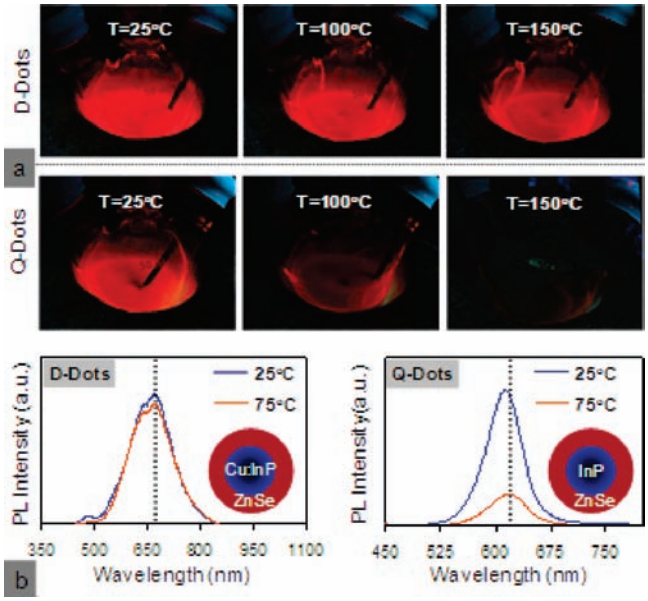

Figure 7. Temperature effects on PL of Cu:InP/ZnSe core/shell d-dots compared with InP/ZnSe core/shell q-dots shown by (a) visual observation and (b) spectroscopic demonstration.

avoided because the shell growth temperature, 220 °C, and a long reaction time were both needed for achieving a decent thickness of the shell materials. This reaction temperature is between the critical temperatures of lattice diffusion for Cu:InP and Cu:ZnSe d-dots systems as discussed above. This means that although the ZnSe shell could perform as a diffusion barrier to slow down the elimination of Cu dopants from the d-dots, some additional technique was needed to completely solve this problem. The results in Figure 6 revealed that this challenge could be solved by using the d-dots with a high dopant ion concentration. Although the initial dopant PL QY was relatively low with a high dopant concentration (Figure 4b and Figure 6c), the final dopant PL QY became optimal when some of the dopant ions were eliminated from the d-dots.

Thermal stability of Cu dopant PL of Cu:InP/ZnSe core/shell d-dots was investigated using InP/ZnSe core/shell q-dots with similar ZnSe shell thickness and PL QY as the reference (Figure 7). As reported previously, one of the emission levels for the dopant PL is associated with the Cu atomic levels (Figure 1a), and it should thus be less coupled with lattice vibration in comparison to the excitonic PL, i.e., bandgap PL, of q-dots.

Visually, the d-dots did not show significant change on their dopant PL upon heating up to 150 °C while the reference q-dots demonstrated an almost complete quenching of its bandgap PL (Figure 7a). The emission color of two samples also showed significant difference, with q-dots PL color shifting to red and d-dots showing no noticeable variation upon heating. After heating to 200 °C, the emission intensity of the d-dots also showed some noticeable decrease while the emission color did not change (Figure S7, Supporting Information). All of the changes, both q-dots shown at relatively temperatures and d-dots shown at high temperatures, were found to be reversible. When the samples were cooled down to room temperature, the emission color and intensity for both samples were recovered.

To verify these visual observations in a more quantitative manner, the PL spectra of both solution samples were also recorded at room temperature and 75 °C. As shown in Figure 7b, the PL spectra of the d-dots for both temperatures did not show significant difference. Conversely, the PL spectrum of the q-dots showed a noticeable red-shift and substantial decrease of the PL intensity.

The results in Figure 7 confirmed that the photoluminescence of the d-dots originated from the doping centers. Different from the well studied Mn:ZnSe d-dots system, the emission of Cu:InP d-dots is actually hybridized combination, with the electron from the conduction band hole from the Cu dopant center (Figure 1a). The above results revealed that such a system still behaves more like pure dopant emission, instead of bandgap emission in terms of the temperature dependence. The outstanding thermal, stability of the Cu:InP/ZnSe core/shell d-dots further implies that these d-dots are more capable for some special technical applications than are the corresponding q-dots, for which high temperature is inevitable, such as solid-state lighting, lasers,[37] light-emitting diodes,[38,39] etc.

Conclusion

In summary, high qualtiy Cu:InP and Cu:InP/ZnSe core/shell d-dots were successfully synthesized by exploring several key aspects of the related synthetic chemistry, including reaction temperature profile, dopant concentration, and an epitaxially grown ZnSe shell as the diffusion barrier, etc. The PL QY of the resulting Cu:InP/ZnSe core/shell d-dots, as the first example of d-dots emitters based on III−V host nanocrystals, reproducibly reached close to 40% and the corresponding emission peak could be tuned from 630 to 1100 nm, which compensates for the existing high performance d-dots based on ZnSe hosts as non-cadmium nanocrystal emitters. In comparison to the d-dots based on II−VI semiconductor nanocrystals, Cu:InP d-dots were found to be more vulnerable toward chemical oxidation, dopant diffusion, and nonradiative decay upon photoexcitation. Results reveal that all of these problems could be solved by the epitaxy growth of a few monolayers of ZnSe shell using the one-pot approach demonstrated in this report. The pure and efficient dopant PL of the resulting Cu:InP/ZnSe core/shell d-dots was found to possess all of the expected advantages of d-dots emitters, i.e., outstanding thermal stability, no overlapping of the absorption and PL to avoid self-quenching, and acceptable chemical stability.

Experimental Section

Materials. Technical grade (90%) octadecene (ODE), indium acetate ($In(Ac)_3$, 99.99%), tri-*n*-octylphosphine (TOP, 97%), stearic acid (SA, 98%), oleic acid (90%), zinc stearate (ZnO 12.5−14%), tris(trimethylsilyl)phosphine ($P(TMS)_3$, 95%), and 1-octylamine (99%) were purchased from Alfa. Oleylamine (97%) was purchased from Aldrich. Copper stearate was prepared in our lab. All the chemicals were used without further purification.

Synthesis of Cu:InP Nanocrystals. The injection solution of P precursor was prepared by mixing 0.2 mmol of tris(trimethylsilyl)phosphine and 2.4 mmol of ODE (1.5 mL in total) in a glovebox. For a typical synthesis, indium acetate (0.4 mM), myristic acid (1.4 mM), and 4 g of 1-octadecene (ODE) were loaded into a three-neck flask. The mixture was heated to 188 °C under argon flow, and then the P precursor solution made in the glovebox was injected into the hot reaction mixture, which lowered the reaction temperature to 178 °C for 10 min. The reaction solution was further cooled

(37) Lee, J.; Sundar, V. C.; Heine, J. R.; Bawendi, M. G. *J. Am. Chem. Soc.* **2000**, *122*, 1102.
(38) Colvin, V. L.; Schlamp, M. C.; Alivisatos, A. P. *Nature* **1994**, *370*, 354.
(39) Klimov, V. I.; Ivanov, S. A.; Nanda, J.; Achermann, M.; Bezel, I.; McGuire, J. A.; Piryatinski, A. *Nature* **2007**, *447*, 441.

to 130 °C, and the copper precursor solution (0.02 mmol of copper stearate in ODE) was added into the reaction solution. The reaction mixture was further heated to 210 °C for the doping of InP nanocrystals with Cu ions with a heating rate of about 2 °C/min. This entire process was monitored through UV−vis and PL measurements by taking aliquots from the reaction mixture at a given time/temperature dissolved in toluene. Some chosen aliquots were further examined using TEM, EDX, and electron diffraction. EDX was performed after the aliquots were purified by ethanol. The same purification procedure was performed for the core/shell samples for EDX measurements. For the growth of Cu:InP/ZnSe core/shell nanocrystals, the reaction mixture was used directly without isolation (see details below). For XRD measurements, the reaction mixture was allowed to cool to room temperature and purified by adding ethanol into the solution, and the solid product was finally isolated by centrifugation, decantation, and drying under Ar flow.

One-Pot Synthesis of Cu:InP/ZnSe Core/Shell Nanocrystals. For the epitaxial growth of ZnSe shell, the reaction solution made in the above paragraph was cooled down to 150 °C. Zinc stearate (0.1 M in ODE) and selenium (0.1 M in TOP) precursor solutions (1.2 mL each) were separately added into the reaction flask, with a 10 min time interval between the two injections at 150 °C. After that, the temperature was increased to 220 °C for 30 min to allow the growth of the ZnSe shell. The reaction mixture was again cooled to 150 °C for the addition of the precursor solutions with a different amount (1.65 mL each for the second run of SILAR) and was heated to 220 °C for 30 min to grow an additional layer of ZnSe shell. Similarly, for the third (2.1 mL of each precursor solution), fourth (2.8 mL of each precursor solution), and fifth (3.5 mL of each precursor solution of ZnSe shell epitaxy), the temperature always followed the same "thermal cycling" settings, 150 °C for the addition of the precursor solutions and 220 °C for the growth of the shell. The entire shell epitaxy process was monitored by taking aliquots for UV−vis, PL, TEM, electron diffraction, EDX, and measurement. When the synthesis was completed, the reaction was allowed to cool to room temperature. For purification, 10 mL of hexane was added to the reaction solution, and the unreacted starting materials and byproducts were removed by successive methanol extractions until the methanol phase was clear. The solid form of the Cu:InP/ZnSe core/shell d-dots was isolated by the addition of acetone into the purified hexanes/ODE solution, followed by centrifugation, decantation, and drying under Ar flow. The resulting core/shell d-dots can be dispersed in organic solvents, such as chloroform and toluene.

The effects of dopant concentration were studied using the same procedure described in the above subsections except that a different amount of the Cu precursor was added into the reaction solution at 180 °C for UV−vis and PL measurements.

Thermal Stability of d-dots and q-dots. Purified Cu:InP/ZnSe and InP/ZnSe core/shell nanocrystals were dispersed in ODE, and the solutions were heated from room temperature to different temperatures, up to 300 °C, under argon. The digital pictures were taken with a fixed position and elimination conditions for a given sample in the flask. The PL spectra at different temperatures were taken in situ using a temperature control unit (up to 80 °C) attached to a Spex Fluorolog-3 fluorometer.

Transmission Electron Microscopy (TEM) and High Resolution TEM (HR-TEM). The low-resolution TEM images were taken on a JEOL 100CX transmission electron microscope with an acceleration voltage of 100 kV. Carbon-coated copper grids were dipped in the hexanes or toluene solutions to deposit nanocrystals onto the film. High-resolution TEM (HRTEM) pictures were taken using a Taitan microscope with an acceleration voltage of 300 kV.

The PL QY Measurement of d-Dots. There is no a reference dye for d-dots because of their unusually large Stokes shift. Therefore, we used InAs quantum dots as the intermediate reference. The PL QY of the Cu:InP d-dots were calculated by the comparison of the fluorescence intensity with InAs QDs with the same optical density at the excitation wavelength and similar fluorescence wavelength.

The Other Measurements. X-ray powder diffraction (XRD) patterns were obtained using a Philips PW1830 X-ray diffractometer. Energy-dispersive spectroscopy (EDS) was used for elemental analysis using a Philips ESEM XL30 scanning electron microscope equipped with a field emission gun and operated at 10 kV. UV−vis spectra were recorded on an HP8453 UV−visible spectrophotometer. Photoluminescence (PL) spectra were taken using a Spex Fluorolog-3 fluorometer.

Acknowledgment. This work was partially supported by the NSF and NIH. We thank M. Rutherford for assistance on EDS and XRD measurements.

Supporting Information Available: Supporting results mentioned in the text are available free of charge via the Internet at http://pubs.acs.org.

JA903558R